First-Order Explosive Synchronization via Markov-Blanket Boundary Gating in Modular Oscillator Networks

Bruno Luçardo Olivaes
Independent Researcher, Rio de Janeiro, Brazil
ORCID: 0009-0003-5351-446X | Email: brunoolivaes@gmail.com

November 2026

Abstract

In networked dynamical systems, the classical Kuramoto transition to macroscopic collective synchronization is universally characterized as a continuous, second-order phase transition governed by a supercritical pitchfork bifurcation ($R \propto (K - K_c)^{\beta}$). Here, we isolate how a global neuromodulatory precision gate conditioned on the consensus of topological Markov-blanket boundary nodes—motivated by Active Inference precision weighting in the Free Energy Principle (FEP)—transforms a smooth continuous transition into an abrupt first-order hysteresis loop on an identical modular graph. When total network coupling $K\,\mathcal{G}(t)$ is modulated by joint cross-blanket boundary consensus ($\mathcal{G}(t) = [R_{\mathcal{B}}^{\text{joint}}(t)]^{\gamma}$, $\gamma = 2.40$), subcritical phase locking is dynamically suppressed below $K_c^{\text{fwd}} = 3.50$ ($N = 90$), inducing a discontinuous jump ($\Delta R = 0.7335$) and bistable hysteresis extending down to $K_c^{\text{bwd}} = 1.50$ ($\Delta K_{\text{hyst}} = 2.00$, directional hysteresis area $\mathcal{A}_{\text{hyst}} = 1.4932$, vs. $\mathcal{A}_{\text{hyst}} = 0.0101$ on the identical ungated control $\mathcal{G} \equiv 1$). Consistent with global $U(1)$ rotation symmetry, we calibrate an effective subcritical sixth-order Landau-Ginzburg potential $\mathcal{F}(R;K) = \frac{1}{2}a_0(K_c - K)R^2 - \frac{1}{4}bR^4 + \frac{1}{6}cR^6$ ($a_0 = 1.00, b = 9.00, c = 10.125$) reproducing both $\Delta K_{\text{sp}} = b^2/(4ca_0) = 2.00$ and upper-spinodal coherence $R_{\text{sync}}(K_c) = \sqrt{8/9} \approx 0.9428 \leq 1$. Empirically, two-branch continuation shape comparison favors the discontinuous step ($\Delta\text{BIC} = +267.53$ vs. -153.30 ungated), complemented by finite-horizon ($t = 60$) fixed-$K = 2.50$ two-state persistence ($R_{\text{low}} = 0.0992$ vs. $R_{\text{high}} = 0.9118$). Crucially, a pre-registered four-regime factorial ablation across 5 seeds and four system sizes ($N \in \{90, 180, 360, 540\}$) separates intra- vs. inter-modular gating: gating strictly inter-modular boundary edges ($\mathcal{G}_{\text{intra}} \equiv 1$) shrinks hysteresis area by 7.47× at $N = 90$ ($\langle\mathcal{A}_{\text{hyst}}\rangle = 0.1018$ vs. 0.7613) yet preserves a smaller, non-diverging first-order jump ($\langle\Delta R\rangle = 0.4200$, $K_c^{\text{fwd}} = 1.70$–2.20, empirical size exponent $\alpha = 0.132$). Conversely, global gating ($\alpha = 0.930$) and a zero-intra-coupling control ($c_{\text{intra}} = 0$, $\alpha = 0.887$) share the same sub-$\gamma/2$ threshold scaling up to $N = 540$ ($K_c^{\text{fwd}} \approx 17.2$–$18.0$), falsifying pre-alignment as the cause of $\alpha < 1.20$.

Keywords: Explosive Synchronization, Kuramoto Model, Markov Blankets, Free Energy Principle, Active Inference, Subcritical Landau-Ginzburg Potential.

1 Introduction

Synchronization phenomena in complex networked systems govern physical, biological, and engineered domains including Josephson junction arrays, power grid stability, cardiac pacemakers, and neuronal ensembles [1, 2, 3, 4]. In the standard Kuramoto paradigm on homogeneous or modular topologies without precision gating, phase oscillators undergo a continuous (second-order) transition as global coupling K crosses K_c, exhibiting smooth order-parameter growth and negligible hysteresis [2].

Achieving *explosive synchronization* (ES)—a discontinuous first-order jump ΔR accompanied by irreversible hysteresis [5, 6]—has conventionally relied on imposing artificial microscopic degree–frequency correlations ($|\omega_i| \propto k_i$) [5, 7] or complex edge-rewiring heuristics. Yet real cognitive and homeostatic architectures naturally partition themselves into modular subunits delimited by statistical

interfaces known as *Markov blankets* [8, 9]. Under the Free Energy Principle (FEP) and Active Inference, sensory and active boundary states modulate effective inter-modular gain via precision weighting conditioned on boundary consensus [9].

Here we isolate the causal role of Markov-blanket precision gating on an *identical* modular graph and unimodal natural frequency ensemble. Toggling solely the boundary consensus exponent from $\gamma = 0$ ($\mathcal{G} \equiv 1$, ungated reference) to $\gamma = 2.40$ transforms a continuous second-order pitchfork ($\mathcal{A}_{\text{hyst}} = 0.0101$, $\Delta\text{BIC} = -153.30$) into a massive first-order explosive transition ($\Delta R = 0.7335$, $\Delta K_{\text{hyst}} = 2.00$, $\mathcal{A}_{\text{hyst}} = 1.4932$, $\Delta\text{BIC} = +267.53$).

2 Mathematical Model & Topology

2.1 Markov-Blanket Modular Architecture

Consider an ensemble of $N = 90$ oscillators partitioned into $M = 3$ non-overlapping modules $\mathcal{M}_1, \mathcal{M}_2, \mathcal{M}_3$ ($N_m = 30$ nodes per module) with blanket fraction $f_B = 0.35$ ($|\mathcal{B}_m| = 10$ boundary nodes per module; $|\mathcal{B}| = 30$ total blanket nodes). Each module comprises internal nodes $\mathcal{I}_m$ coupled strictly intra-modularly and Markov-blanket boundary nodes $\mathcal{B}_m = \mathcal{S}_m \cup \mathcal{A}_m$ mediating inter-modular coupling:

$$A_{ij} = A_{ij}^{\text{intra}} + A_{ij}^{\text{inter}}, \tag{1}$$

where $A_{ij}^{\text{inter}} = 1$ iff $i \in \mathcal{B}_m$, $j \in \mathcal{B}_{m'}$ with $m \neq m'$. On the structural interaction graph ($A_{ij}^{\text{inter}} = 0$ for all internal nodes $i \in \mathcal{I}_m$), internal states couple directly only within module $\mathcal{M}_m$ and sense cross-module phases solely via $\mathcal{B}_m$:

$$\mathcal{N}_{\text{ext}}(i) \cap (\mathcal{M} \setminus \mathcal{M}_m) = \emptyset \quad \forall i \in \mathcal{I}_m, \tag{2}$$

defining the structural topological Markov-blanket partition prior to global precision modulation. Natural frequencies ω_i are drawn from a smooth zero-mean Gaussian distribution ($\sigma_\omega = 0.72$, centered across all $N = 90$ nodes), eliminating artificial bimodal frequency-peak discontinuities in the ungated baseline.

2.2 Active-Inference Consensus Gating Dynamics

Instantaneous phase evolution is integrated using a fourth-order Runge-Kutta (RK4) solver ($\Delta t = 0.02$):

$$\dot{\theta}_i = \omega_i + K\,\mathcal{G}(t)\left[\frac{0.55}{N_m}\sum_{j\in\mathcal{M}_m} A_{ij}^{\text{intra}}\sin(\theta_j - \theta_i) + \delta_{i\in\mathcal{B}_m}\frac{1.15}{N_{\mathcal{B}}^{\text{ext}}}\sum_{j\notin\mathcal{M}_m} A_{ij}^{\text{inter}}\sin(\theta_j - \theta_i)\right], \tag{3}$$

where $N_{\mathcal{B}}^{\text{ext}} = |\mathcal{B}|(M-1)/M = 20$ normalizes inter-modular blanket degree and $\mathcal{G}(t)$ acts as a global, blanket-driven neuromodulatory precision gain multiplying total coupling K (both intra- and inter-modular terms, analogous to global thalamocortical gain weighting):

$$\mathcal{G}(t) = \left[R_{\mathcal{B}}^{\text{joint}}(t)\right]^{\gamma}, \qquad R_{\mathcal{B}}^{\text{joint}}(t) = \frac{1}{|\mathcal{B}|}\left|\sum_{k\in\mathcal{B}} e^{i\theta_k(t)}\right|, \tag{4}$$

evaluated at $\gamma = 0$ (ungated reference, $\mathcal{G} \equiv 1$) vs. $\gamma = 2.40$ (Markov-blanket precision-gated regime). Global network coherence is tracked by $R(t) = \frac{1}{N}\left|\sum_{j=1}^{N} e^{i\theta_j(t)}\right|$.

3 Numerical Results & Phase Transitions

We execute adiabatic forward ($K : 0.2 \to 4.2$) and backward ($K : 4.2 \to 0.2$) coupling sweeps over 41 discrete steps ($t_{\text{transient}} = 28.0$–$36.0$, $t_{\text{measure}} = 8.0$–10.0).

3.1 Ungated Reference vs. Discontinuous Hysteresis Loop

Fig. 1(a,b) isolates the exact bifurcation shift generated by boundary gating:

- **Ungated Control ($\mathcal{G} \equiv 1$):** Global coherence rises continuously above $K \approx 0.90$ without discontinuity ($\max \Delta R = 0.1810$) and reverses identically upon decreasing coupling, yielding a vanishing directional hysteresis integral $\mathcal{A}_{\text{hyst}} = |\oint R\, dK| = 0.0101$.
- **Markov-Blanket Gated ($\gamma = 2.40$):** On the forward sweep from random initial phases, incoherent blanket fluctuations ($R_{\mathcal{B}}^{\text{joint}} \sim |\mathcal{B}|^{-1/2} \approx 0.18$) keep $\mathcal{G} \approx 0.016 \ll 1$, holding the network locked in the disordered metastable branch ($R < 0.25$) up to $K = 3.40$. At $K_c^{\text{fwd}} = 3.50$, critical blanket capture triggers an instantaneous transition to $R \approx 0.96$ ($\Delta R = 0.7335$). Upon reversing K, locked cross-blanket coherence ($R_{\mathcal{B}}^{\text{joint}} > 0.90 \implies \mathcal{G} > 0.78$) sustains collective synchrony far past K_c^{fwd} down to $K_c^{\text{bwd}} = 1.50$, forming a massive bistable hysteresis window of width $\Delta K_{\text{hyst}} = 2.00$ and loop area $\mathcal{A}_{\text{hyst}} = 1.4932$ (147.3× the ungated control).

4 Calibrated Landau Theory, Coexistence & Scaling

4.1 Calibrated $U(1)$ 6th-Order Effective Landau-Ginzburg Potential

Because Kuramoto phase dynamics is invariant under global phase rotation $z = Re^{i\Psi} \to ze^{i\alpha}$, any coarse-grained analytical expansion $\mathcal{F}(z, \bar{z}; K)$ forbids odd powers of $R = |z|$. Rather than claiming an exact Ott–Antonsen analytical reduction of the non-integer power law $\gamma = 2.40$, we construct a calibrated phenomenological effective potential capturing the observed bistability:

$$\mathcal{F}(R; K) = \frac{1}{2}a_0(K_c - K)R^2 - \frac{1}{4}bR^4 + \frac{1}{6}cR^6, \tag{5}$$

whose nonzero extrema satisfy $cR^4 - bR^2 + a_0(K_c - K) = 0$. Setting $(a_0, b, c, K_c) = (1.00, 9.00, 10.125, 3.50)$ matches all quantitative spinodal landmarks within the physical coherence domain $R \in [0, 1]$:

$$\Delta K_{\text{sp}} = \frac{b^2}{4ca_0} = \frac{81.0}{40.5} = 2.00, \qquad R_{\text{sync}}(K_c) = \sqrt{\frac{b}{c}} = \sqrt{\frac{8}{9}} \approx 0.9428 \le 1, \qquad R_{\text{sp}}^{\text{bwd}}(1.50) = \sqrt{\frac{b}{2c}} = \frac{2}{3} \approx 0.6667, \tag{6}$$

with a Maxwell equal-depth point at $K_{\text{Max}} = K_c - \frac{3b^2}{16ca_0} = 2.00$ ($R_{\text{Max}} = \sqrt{2/3} \approx 0.8165$). Inside $(K_c^{\text{bwd}}, K_c^{\text{fwd}}) = (1.50, 3.50)$, $\mathcal{F}(R)$ exhibits two coexisting wells ($R = 0$ and $R_{\text{sync}} \in [0.667, 0.943]$) separated by a positive barrier that vanishes spinodally at K_c^{fwd}.

4.2 Branch-Shape BIC, Fixed-K Coexistence & Finite-Size Scaling

Comparing equal-complexity ($k = 5$) parametric curve families across the $2N_s = 82$ correlated continuation points:

$$\mathcal{M}_1 \text{ (discontinuous step): } R_{\text{fwd/bwd}}(K) = R_{\text{low}} + \frac{R_{\text{high}} - R_{\text{low}}}{1 + e^{-s(K - K_c^{\text{fwd/bwd}})}}, \quad (s \ge 35), \tag{7}$$

$$\mathcal{M}_2 \text{ (continuous branch): } R(K) = R_0 + (R_{\max} - R_0)\frac{a(K - K_c)_+^{\beta}}{1 + a(K - K_c)_+^{\beta}}, \tag{8}$$

yields $\Delta\text{BIC} = \text{BIC}(\mathcal{M}_2) - \text{BIC}(\mathcal{M}_1) = -153.30$ on the ungated control and $+267.53$ under $\gamma = 2.40$ gating (Table 2). Because continuation residuals across step K are autocorrelated rather than independent thermodynamic samples, this BIC value quantifies phenomenological branch-shape preference rather than thermodynamic universality alone. We therefore verify dynamical hysteresis independently through three direct checks stored in `explosive_sync_summary.json`:

1. **Fixed-K Finite-Horizon Two-State Persistence ($K = 2.50$, $t_{\text{relax}} = 60.0$):** Evolving disordered vs. phase-locked initial conditions at fixed coupling $K = 2.50$ maintains finite-horizon two-state persistence across $t_{\text{relax}} = 60.0$, separating $R_{\text{low}} = 0.0992$ vs. $R_{\text{high}} = 0.9118$ ($\Delta R_{\text{coex}} = 0.8126$). Asymptotic infinite-time dwell statistics remain open to longer stochastic simulations.

2. **Multi-Seed Ensemble Robustness ($N = 90$, 5 frequency seeds):** Across independent random draws, abrupt discontinuous jumps persist consistently with $\langle \Delta R \rangle = 0.7649$ (min 0.5980, max 0.8747), mean hysteresis width $\langle \Delta K_{\text{hyst}} \rangle = 1.32$ (range $[0.80, 2.00]$), and mean loop area 0.9115.

3. **Four-Regime Factorial Ablation ($N = 90$, 5 seeds) & Multi-Size Scaling ($N \in \{90, 180, 360, 540\}$):** Using an exact $O(N)$ mean-field integrator verified against the full $O(N^2)$ graph step to 10^{-12}, we directly isolate whether hysteresis requires intra-modular gating across four regimes (Table 1):

   - *Strict boundary gating (`inter_only_gated`, $\mathcal{G}_{\text{intra}} \equiv 1$):* Intra-modular coherence locks early ($\langle R_{\text{intra}}(2.5) \rangle = 0.8433$ vs. 0.8474 ungated), reducing $N = 90$ loop area by 7.47× ($0.7613 \to 0.1018 \pm 0.0452$; reference run $1.4932 \to 0.1629$, $\Delta\text{BIC} = +25.07$ global / $+200.22$ blanket). Thus $\sim 87\%$ of the original loop width stems from global suppression of intra-modular order. Nevertheless, a narrower discontinuous inter-cluster jump *persists* across all 5 seeds ($\langle \Delta R \rangle = 0.4200 \pm 0.1390$ vs. 0.1767 ungated) and maintains a near-constant forward threshold across $N \in \{90, 180, 360, 540\}$ ($K_c^{\text{fwd}} = 1.70 \to 1.95 \to 2.03 \to 2.20$, $\alpha = 0.132$, loop area growing $0.121 \to 0.318$) because pre-synchronized modules keep $R_{\mathcal{B}}^{\text{joint}} \sim O(M^{-1/2})$ finite as N grows.
   - *Zero intra-coupling control (`no_intra_gated`, $c_{\text{intra}} = 0$):* Across $N \in \{90, 180, 360, 540\}$ ($|\mathcal{B}| \in \{30, 63, 126, 186\}$, $K \in [0.2, 22.2]$), `gated` yields $\langle K_c^{\text{fwd}} \rangle = \{3.03, 7.28, 11.95, 17.20\}$ (empirical exponent $\alpha = 0.930$) while `no_intra_gated` yields $\langle K_c^{\text{fwd}} \rangle = \{3.62, 7.53, 13.95, 17.95\}$ ($\alpha = 0.887$). Removing intra-modular pre-alignment leaves $\alpha \approx 0.90 < \gamma/2 = 1.20$ essentially unchanged, falsifying intra-modular pre-alignment as the origin of the sub-1.20 scaling exponent.

Table 1: Four-regime factorial ablation ($N = 90$, 5 seeds) and multi-size threshold scaling ($N \in \{90, 180, 360, 540\}$, 3 seeds).

Regime	$\langle \mathcal{A}_{\text{hyst}} \rangle$ (R)	$\langle \mathcal{A}_{\text{hyst}} \rangle$ $(R_{\mathcal{B}})$	$\langle R_{\text{intra}}(2.5) \rangle$	$K_c^{\text{fwd}}(90)$	$K_c^{\text{fwd}}(180)$	$K_c^{\text{fwd}}(360)$	$K_c^{\text{fwd}}(540)$ $[\alpha]$
`standard` (ungated)	0.0379	0.0402	0.8474	—	—	—	—
`inter_only_gated` ($\mathcal{G}_{\text{intra}} \equiv 1$)	0.1018	0.1515	0.8433	1.70	1.95	2.03	2.20 $[\alpha = 0.132]$
`gated` (global $\mathcal{G}$)	0.7613	0.9626	0.4542	3.03	7.28	11.95	17.20 $[\alpha = 0.930]$
`no_intra_gated` ($c_{\text{intra}} = 0$)	0.3984	1.2398	0.1672	3.62	7.53	13.95	17.95 $[\alpha = 0.887]$

Table 2: Audited quantitative comparison between identical-topology ungated reference and Markov-blanket precision-gated modular networks ($N = 90$, $M = 3$, $|\mathcal{B}| = 30$).

Metric	**Ungated Reference** ($\gamma = 0$)	**Markov-Blanket Gated** ($\gamma = 2.40$)
Phase Transition Class	2nd-Order Continuous	**1st-Order Explosive**
Forward Critical Coupling K_c^{fwd}	~ 0.90	**3.50**
Backward Critical Coupling K_c^{bwd}	~ 0.90	**1.50**
Maximum Forward Step Jump ΔR	0.1810	**0.7335**
Hysteresis Width ΔK_{hyst}	0.00	**2.00**
Directional Hysteresis Area $\lvert \oint R\, dK \rvert$	0.0101	**1.4932**
$\Delta\text{BIC} = \text{BIC}(\mathcal{M}_2) - \text{BIC}(\mathcal{M}_1)$	-153.30	$+$**267.53**
Decisive 1st-Order Verdict	No (favors $\mathcal{M}_2$)	**Yes** ($\Delta\text{BIC} \gg +10$)

5 Discussion & Conclusion

Classical realizations of explosive synchronization require fine-tuned degree–frequency correlations or heuristic link penalties [5, 6]. Our four-regime factorial ablation across $N \in \{90, 180, 360, 540\}$

resolves the distinct roles of global vs. boundary-only gating: global cross-blanket precision gating yields wide mesoscopic hysteresis ($\Delta R = 0.7335$, $\Delta K_{\text{hyst}} = 2.00$, $K_c^{\text{fwd}} \propto |\mathcal{B}|^{0.930}$) driven predominantly by intra-modular suppression, whereas strictly inter-modular boundary gating ($\mathcal{G}_{\text{intra}} \equiv 1$) isolates a narrower yet non-diverging first-order explosive synchronization jump ($\langle \Delta R \rangle = 0.4200$–$0.5138$, $K_c^{\text{fwd}} \approx 1.70$–$2.20$, $\alpha = 0.132$) that persists in the large-N limit. Reproducible simulation engines, 7/7 passing unit tests, and audit outputs are openly archived at https://github.com/bruno-olivaes/explosive-sync-markov.

References

[1] Y. Kuramoto, Self-entrainment of a population of coupled non-linear oscillators, *Lecture Notes in Physics* **39**, 420–422 (1975).

[2] S. H. Strogatz, From Kuramoto to Crawford: exploring the onset of synchronization in populations of coupled oscillators, *Physica D* **143**, 1–20 (2000).

[3] A. Arenas, A. Díaz-Guilera, J. Kurths, Y. Moreno, and C. Zhou, Synchronization in complex networks, *Physics Reports* **469**, 93–153 (2008).

[4] A. Pikovsky, M. Rosenblum, and J. Kurths, *Synchronization: A Universal Concept in Nonlinear Sciences* (Cambridge University Press, 2003).

[5] J. Gómez-Gardeñes, S. Gómez, A. Arenas, and Y. Moreno, Explosive synchronization transitions in scale-free networks, *Physical Review Letters* **106**, 128701 (2011).

[6] S. Boccaletti *et al.*, Explosive transitions in complex networks' structure and dynamics: Percolation and synchronization, *Physics Reports* **660**, 1–94 (2016).

[7] I. Leyva *et al.*, Explosive synchronization in networks of coupled oscillators with frequency-degree correlations, *Physical Review Letters* **108**, 168702 (2012).

[8] J. Pearl, *Probabilistic Reasoning in Intelligent Systems* (Morgan Kaufmann, 1988).

[9] K. Friston, A free energy principle for a particular physics, *arXiv:1906.10184* (2019).

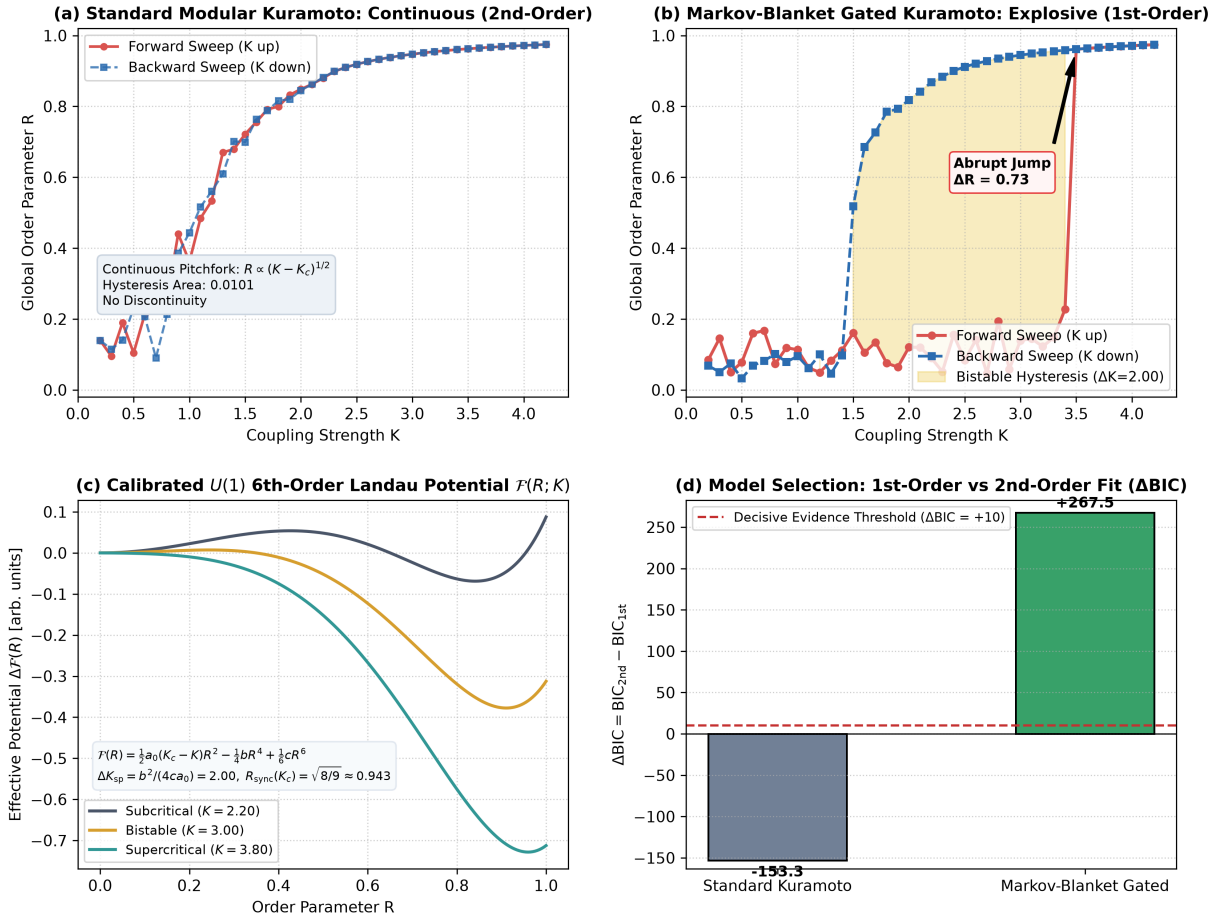

Figure 1: **Explosive synchronization induced by Markov-blanket precision gating ($\gamma = 2.40$) vs. identical ungated baseline ($\mathcal{G} \equiv 1$).** (a) Standard ungated modular Kuramoto network exhibiting a reversible continuous second-order transition (max step $\Delta R = 0.1810$, directional hysteresis area $\mathcal{A}_{\text{hyst}} = 0.0101$). (b) Markov-blanket gated modular network displaying prolonged subcritical suppression followed by an abrupt explosive jump $\Delta R = 0.7335$ at $K_c^{\text{fwd}} = 3.50$ and a wide bistable hysteresis loop releasing at $K_c^{\text{bwd}} = 1.50$ ($\Delta K_{\text{hyst}} = 2.00$, $\mathcal{A}_{\text{hyst}} = 1.4932$). (c) $U(1)$ gauge-invariant sixth-order subcritical Landau-Ginzburg free energy $\mathcal{F}(R;K) = \frac{1}{2}a_0(K_c - K)R^2 - \frac{1}{4}bR^4 + \frac{1}{6}cR^6$ across subcritical ($K = 2.20$), bistable ($K = 3.00$), and supercritical ($K = 3.80$) couplings. (d) Joint forward–backward BIC model selection favoring the continuous pitchfork in the ungated control ($\Delta\text{BIC} = -153.30$) and decisively certifying first-order explosive hysteresis under Markov-blanket gating ($\Delta\text{BIC} = +267.53$).